Molecular Microbiology (2004) **51**(5), 1321–1332 doi:10.1046/j.1365-2958.2003.03936.x

MreB, the cell shape-determining bacterial actin homologue, co-ordinates cell wall morphogenesis in *Caulobacter crescentus*

Rainer M. Figge, Arun V. Divakaruni and James W. Gober*
Department of Chemistry and Biochemistry and the Molecular Biology Institute, University of California, Los Angeles, CA 90095-1569, USA.

Summary

The bacterial actin homologue, MreB, is required for the maintenance of a rod-shaped cell and has been shown to form spirals that traverse along the longitudinal axis of *Bacillus subtilis* and *Escherichia coli* cells. The depletion of MreB in *Caulobacter crescentus* resulted in lemon-shaped cells that possessed defects in the integrity of the cell wall. MreB localization appeared as bands or spirals that encircled the cell along its entire length and switched to a mid-cell location at a time that coincided with the initiation of cell division. The formation of smaller MreB spirals or bands at the mid-cell was dependent on the presence on the cytokinetic protein, FtsZ. Penicillin-binding protein 2 (PBP2) also formed band-like structures perpendicular to the cell periphery that resembled, and depended upon, MreB localization. PBP2 co-immunoprecipitated with several other penicillin-binding proteins, suggesting that these proteins are in association in *Caulobacter* cells. We hypothesize that MreB filaments function as a cytoskeleton that serves as an organizer or tracking device for the PBP2–peptidoglycan biosynthesis complex.

Introduction

In many organisms, a major determinant of cellular morphology is the shape of the cell wall. In bacteria, the cell wall, or peptidoglycan layer, serves as a scaffold that reinforces the cell against intracellular osmotic pressure. Isolated cell wall sacculi retain most of the original shape of the organism, an observation that is consistent with the idea that the cell wall confers a distinct shape on the intact cell (Holtje, 1998). For rod-shaped bacteria, morphogenesis occurs in two distinct phases, cell elongation followed by septation (cell division) (Wientjes and Nanninga, 1989; Nanninga, 1991; de Pedro *et al*., 1997). During the elongation phase, the cells grow along the longitudinal axis with little increase in width. Once a critical cell length is attained, cell wall synthesis switches direction at the mid-cell, turning inward, thus forming a cell division septum. The regulation of these two phases in cell wall morphogenesis is co-ordinated with other cell cycle-related events such as DNA replication and chromosome partitioning.

The structure and composition of peptidoglycan has been determined in detail, and many enzymes involved in its synthesis have been characterized (Holtje, 1998). Peptidoglycan consists of a glycan polymer of N-acetylglucosamine and N-acetylmuramic acid that forms a series of chains girdling the circumference of the cell along its entire length. This chain of glycan is given structural integrity through cross-linking via short peptides. A well-characterized class of enzymes required for the assembly of peptidoglycan from intracellularly synthesized precursors is collectively known as penicillin-binding proteins (PBPs) (Holtje, 1998). As their name implies, these enzymes were originally identified as the targets of β-lactam antibiotics (Spratt and Pardee, 1975) and generally fall into two distinct biosynthetic classes. The high-molecular-weight PBPs (i.e. PBP1a, PBP1b) are bifunctional enzymes possessing the capacity to assemble both the glycan chain and the peptide cross-links (Holtje, 1998). In addition to these, most bacteria possess PBPs of lower molecular weight (i.e. PBP2, PBP3) that function solely in assembling peptide cross-links. In rod-shaped bacteria, two of these lower molecular weight PBPs are implicated in directing the two morphogenetic phases of cell growth: cell elongation and cell division (Spratt, 1975; Satta *et al*., 1980). Inactivation of PBP2 (*pbpA*) either through the use of antibiotics or by conditional mutants results in the formation of spherical cells, suggesting that PBP2 is required for cell elongation (Begg and Donachie, 1985). Similar experimental strategies have demonstrated that PBP3 (*ftsI*) is required for peptidoglycan synthesis at the mid-cell

Accepted 11 November, 2003. *For correspondence. E-mail gober@chem.ucla.edu; Tel. (+1) 310 206 9449; Fax (+1) 310 206 5213.

(Nakamura *et al*., 1983) and thus has a critical role in the formation of the cell division septum (Ishino *et al*., 1989). It is currently not known how the cell switches from PBP2 activity to PBP3 activity at a specific time during the cell cycle.

In addition to *pbpA* (PBP2), several other genes encoding proteins that do not directly catalyse cell wall synthesis have been shown to play an important role in the determination of the rod-shape in *Bacillus subtilis* (Levin *et al*., 1992; Varley and Stewart, 1992) and *Escherichia coli*. Mutations in *rodA* (Spratt, 1975; Tamaki *et al*., 1980), which encodes an integral membrane protein, as well as mutations in each gene of the *mreBCD* gene cluster results in round-shaped *E. coli* cells (Wachi *et al*., 1987; Doi *et al*., 1988; Wachi and Matsuhashi, 1989). Furthermore, in *B. subtilis*, *mreB* is essential for survival (Varley and Stewart, 1992). Depletion of MreB from *B. subtilis* cells results in a loss of rod shape over time (Jones *et al*., 2001), indicating that the function of MreB in the maintenance of cell shape is conserved. In support of this idea, examination of completed bacterial genome sequences has revealed that *mreB* is absent from the genomes of coccoid organisms.

MreB is a member of the HSP70–actin–sugar kinase superfamily (Jones *et al*., 2001). Unlike HSP70 and sugar kinases of this family, MreB has been shown to fold into a structure that is strikingly similar to eukaryotic actin (van den Ent *et al*., 2001). MreB was shown to form spirals that traverse the longitudinal axis of *B. subtilis* cells (Jones *et al*., 2001), a finding that suggests that bacteria have an internal actin-like cytoskeleton comparable to eukaryotes that dictates their cell shape. As cell shape in bacteria is generally thought to be determined by the cell wall peptidoglycan layer, the spiral-like MreB structures raise an interesting question; does MreB fulfil a true cytoskeletal role, or does it instead co-ordinate the synthesis of the peptidoglycan cell wall in a way similar to actin activation of cell wall growth in yeast (Pruyne and Bretscher, 2000)?

Here, we investigate the function of the *mreB* gene in the dimorphic bacterium *Caulobacter crescentus*. We demonstrate that *mreB* is an essential gene in *C. crescentus* and has a critical role in determining a rod-like shape. We show that MreB forms spirals, the pattern of which changes in a cell cycle-dependent fashion that parallels the two morphogenetic phases of cell elongation and cell division. In addition, we show that PBP2 forms band-like structures similar to those of MreB, and that these structures are lost in MreB-depleted cells. Immunoprecipitation experiments indicate that PBP2 forms a complex with other penicillin-binding proteins. We hypothesize that intracellular MreB spirals are responsible for spatially co-ordinating the activities of cell wall assembly proteins.

Results

MreB forms intracellular helical-like structures with a pattern that changes dynamically during the Caulobacter *cell cycle*

In order to determine whether the *Caulobacter* MreB protein formed spiral-shaped structures similar to the ones found in *B. subtilis* (Jones *et al*., 2001) and *E. coli* (Shih *et al*., 2003), we performed immunofluorescence microscopy using affinity-purified MreB antibody. Localization of MreB appeared as either spaced bands (Fig. 1A–C), sometimes with an intense staining band near the mid-cell (Fig. 1A, cell labelled with an arrow), or spirals encompassing almost the entire cell circumference when observed from the side (Fig. 1C, cell labelled with an arrow). In order to visualize better and confirm the helical-shaped localization pattern of MreB, we performed deconvolution microscopy (Fig. 1D–I). MreB localization appeared as a helix following the long axis of the cell (Fig. 1D and F) similar to those observed in *B. subtilis* and *E. coli* cells (Jones *et al*., 2001; Shih *et al*., 2003), as a criss-cross pattern (Fig. 1E) or as a series of bands (Fig. 1H). Many of the cells also exhibited strong staining at the mid-cell (Fig. 1G and I). The mid-cell localization was accompanied by localization of variable intensity in other regions of the cell.

The fact that the intracellular spiral-like structures formed by MreB differed in their length and localization pattern prompted us to investigate whether or not these distinct localization patterns changed during the cell cycle. *Caulobacter* cells were synchronized and allowed to progress through the cell cycle. Samples processed for immunofluorescence microscopy at different time points revealed that a concentration of spirals at the mid-cell assembled and disassembled in a dynamic fashion (Fig. 2A). In swarmer cells, i.e. at the beginning of the cell cycle (time = 0 min), spiral-like structures, appearing as either spaced bands or dots, were distributed over the entire cell length (data not shown). At about 60–80 min into the cell cycle, in early predivisional cells, more prominent bands of MreB concentrated to the mid-cell region (Fig. 1J and K) in about 75% of the cells (Fig. 2A) with less intense staining bands distributed along the entire length of the cells. This concentrated localization of MreB remained at mid-cell until the completion of cell division, ≈100–120 min, and then decreased in frequency (Fig. 2A). After cell division, the progeny swarmer and stalked cells possessed only the smaller spiral-like structures distributed along the length of the cell (Fig. 2A).

As changes in MreB patterns may be the result of differences in MreB concentrations during the cell cycle, we determined the rate of MreB synthesis and the amount of protein present in synchronized cells. Pulse labelling of protein and subsequent immunoprecipitation of MreB

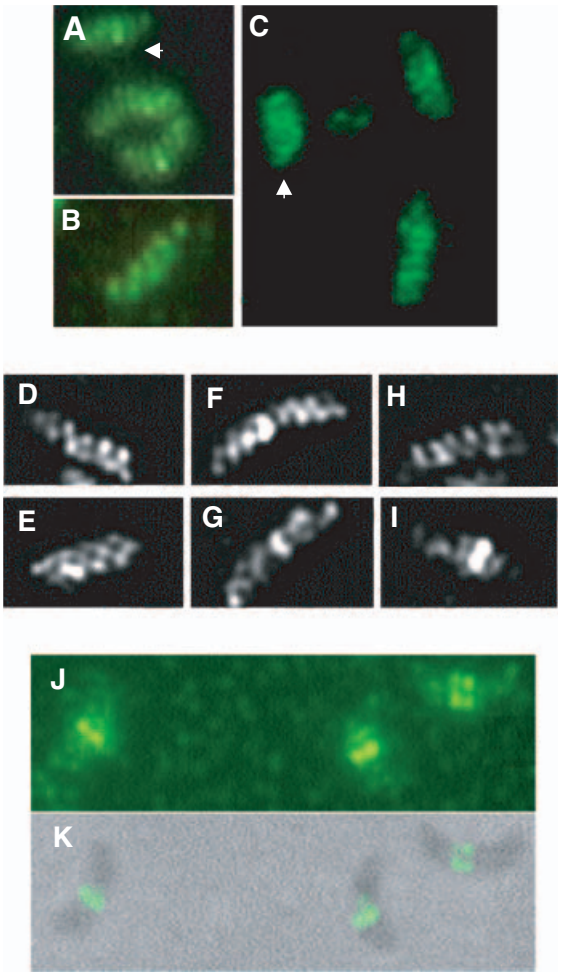

Fig. 1. MreB localizes in a spiral-like pattern in *Caulobacter crescentus* cells.
A–C. Immunostaining of MreB with affinity-purified rabbit antibodies and secondary antibody coupled to the fluorophore Cy3 in cells from unsynchronized cultures. The images are false-coloured in green. When viewed from above, the entire length of the cell, MreB localization appears as a series of bands that are perpendicular to the cell border or as more intense localization at the mid-cell (A – arrow). In a cell that is viewed from the end, MreB appears to be localized as a helical filament (C – arrow).
D–I. Images of MreB immunostaining obtained after deconvolution microscopy in cells from unsynchronized cultures. Localization appears as a helical or coiled shape along the long axis of the cell (D) and (F), a criss-cross pattern (E) or a banded pattern (H) similar to that observed using conventional microscopy. In addition, a band at the mid-cell is observed in some cells with either accompanying helical localization along the cell length (F) or less intense staining in non-mid-cell regions (G) and (I).
J and K. MreB localization at the mid-cell in a synchronized population of predivisional cells. A pure population of swarmer cells was isolated and permitted to progress through the cell cycle. At different times, samples were removed and processed for immunofluorescence microscopy using affinity-purified anti-MreB antibody. Early in the cell cycle, MreB staining appears as a series of bands perpendicular to the cell periphery along the longitudinal axis similar to the pattern presented above (A–D and H) (data not shown). Between 60 and 100 min, corresponding to the predivisional stage, MreB localization appears at the mid-cell (J) (90 min sample).
K. Fluorescence image from (J) superimposed on a phase-contrast image of the same field.

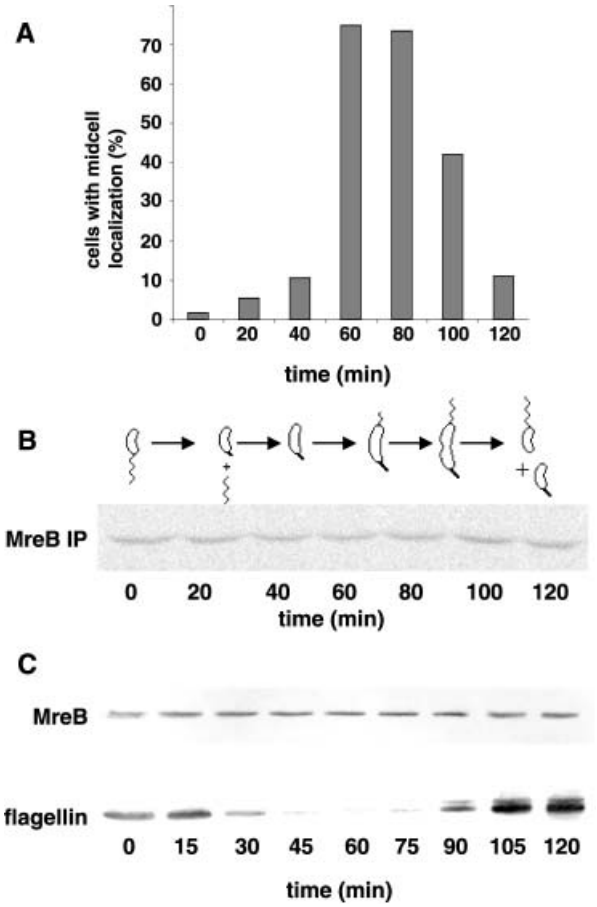

Fig. 2. MreB undergoes dynamic pattern of subcellular localization during the *Caulobacter* cell cycle.
A. A synchronized population of *C. crescentus* cells was followed through the cell cycle (120 min). Samples taken at the time intervals indicated were subjected to MreB immunofluorescence microscopy. A graph depicting the percentage of cells with a mid-cell concentration of MreB localization is shown during the course of the *Caulobacter* cell cycle. At least 100 cells from two independent experiments were counted at each time point, and the percentage of cells with predominant mid-cell localization was determined. MreB localization concentrates at the mid-cell at a time coinciding with the initiation of cell division (60–100 min) (see Fig. 1J). Late in the cell cycle, the centre concentration of MreB localization disappears, leaving cells possessing a spiral-like pattern of localization along the cell length.
B. MreB expression does not change during the course of the cell cycle. *Caulobacter* cells were synchronized and allowed to progress through the cell cycle. At the indicated times, a portion of the culture was removed, and proteins were pulse labelled with ^{35}S-*trans*-label. Labelled MreB was immunoprecipitated, subjected to electrophoresis and visualized by a phosphorimager. Cell types present at each time point, as assayed by light microscopy, are represented schematically above the gel.
C. MreB protein levels remain constant during the cell cycle. The level of MreB in a synchronized culture was determined by immunoblot using anti-MreB antibody. Samples were taken at the indicated time points. As a control, the same immunoblot was also probed with antiflagellin antibody.

showed that the rate of MreB synthesis did not change during the cell cycle (Fig. 2B). Similarly, the amount of MreB protein present at different times during the cell cycle remained constant (Fig. 2C). Thus, the dynamic changes in MreB localization during the cell cycle are not caused by changes in the MreB concentration.

Mid-cell spiral formation is dependent on the cell division protein FtsZ

The appearance of MreB at mid-cell coincided with the initiation of cell division. The earliest known event in the initiation of cell division in bacteria is the formation of a ring of FtsZ protein at the mid-cell, which, in turn, recruits other proteins involved in cytokinesis (Margolin, 2000). We tested whether the localization of MreB bands at mid-cell was dependent on FtsZ. In order to accomplish this, a *Caulobacter* strain harbouring FtsZ under the control of the inducible xylose promoter (YB1585) (Wang *et al*., 2001) was grown in the presence of xylose, synchronized and the resulting swarmer cell population was cultured in either the presence or absence of inducer. As FtsZ is proteolysed in swarmer cells (Kelly *et al*., 1998), only a low background level of the protein was present in the synchronized populations of swarmer cells (Fig. 3C) (compare with Fig. 5). The remainder of the FtsZ was also turned over during further growth in the absence of inducer. Samples prepared for immunofluorescence microscopy at 30 min intervals following the isolation of swarmer cells and FtsZ depletion revealed that the presence of FtsZ is required for the formation of centrally localized MreB (Fig. 3A). After 60 min into the cell cycle, only 4% of the FtsZ-depleted cells possessed a concentration of MreB at the mid-cell in cells depleted of FtsZ (Fig. 3B), whereas 75% of wild-type cells had bright mid-cell staining (see Fig. 2A). Interestingly, the depletion of FtsZ led to an accumulation of MreB at the poles of some cells (up to 20%) and a more punctate staining pattern along the cell length compared with wild-type cells. This same strain grown in the presence of xylose retained the ability to localize MreB at the mid-cell after 60–90 min (data not shown). MreB levels were unchanged during the course of FtsZ depletion, indicating that the absence of centrally located spirals was not caused by changes in the intracellular MreB concentration (Fig. 3C).

Subcellular distribution of MreB

The MreB helical-like banding pattern in *Caulobacter* suggests that a significant portion of MreB would be polymerized within the cells. As actin can be pelleted by ultracentrifugation if present as polymerized filaments, we attempted to isolate MreB by ultracentrifugation of cleared cell lysates (Fig. 4). Indeed, we found that the majority of

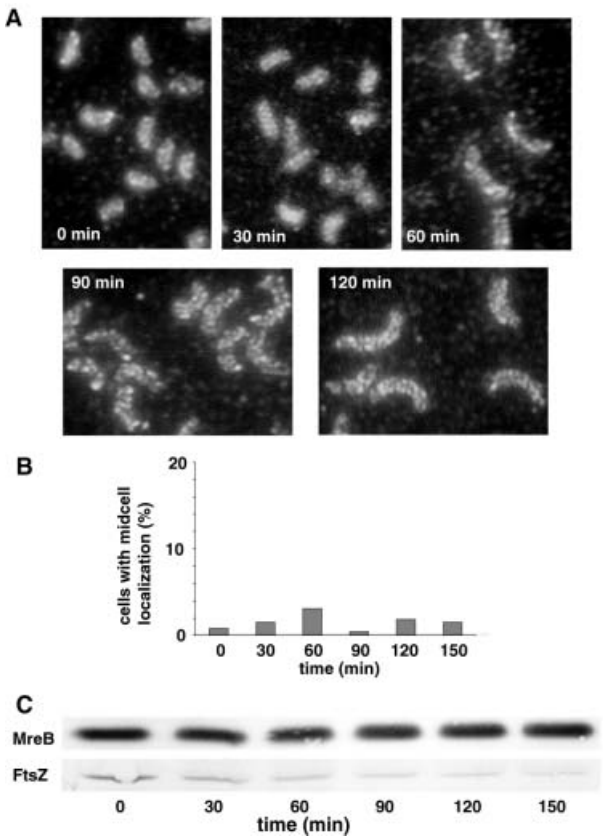

Fig. 3. MreB localization at mid-cell depends on the presence of the cell division protein FtsZ.
A. Swarmer cells of the *C. crescentus* FtsZ depletion strain YB1585 were isolated, and the culture was permitted to progress synchronously through the cell cycle in the absence of inducer (xylose). Samples taken at the indicated time points were subjected to MreB immunofluorescence microscopy. In contrast to wild-type cells, FtsZ depletion abolishes the concentration of MreB localization at the mid-cell.
B. The graph depicts the percentage of cells with a mid-cell concentration of MreB localization during FtsZ depletion in the course of one *Caulobacter* cell cycle. At least 100 cells from two independent experiments were counted at each time point, and the percentage of cells with mid-cell localization was determined.
C. Immunoblot depicting MreB and FtsZ levels upon FtsZ depletion. At the indicated time points after synchronization, samples were removed, proteins were separated by gel electrophoresis, and MreB and FtsZ were visualized by immunoblotting.

MreB was present in the pellet after ultracentrifugation of cell extracts (Fig. 4, lane 3). This pelleted fraction also included cytoplasmic membrane, as indicated by the presence of the integral membrane chemoreceptor, McpA (Fig. 4, lane 3). Sequence composition reveals that MreB is clearly not an integral membrane protein, although it might be peripherally associated with the membrane. We investigated this idea by treating the membrane fraction with sodium carbonate, which removes peripherally associated proteins (Koehler *et al*., 1998). After treatment with sodium carbonate, followed by ultracentrifugation, MreB remained in the pellet fraction (Fig. 4, lane 4) and was not

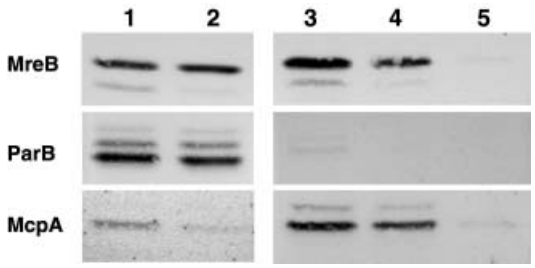

Fig. 4. Subcellular fractionation of MreB. Extracts of *C. crescentus* cells were subjected to subcellular fractionation as described in *Experimental procedures*. After SDS-PAGE, the gels were analysed by immunoblot using the indicated antibodies: anti-MreB, anti-ParB (cytosolic protein; Mohl and Gober, 1997), anti-McpA (integral membrane protein). Lane 1, unfractionated cell extracts; lane 2, cytosolic and periplasmic fraction; lane 3, membrane fraction; lane 4, membrane fraction after treatment with 100 mM Na_2CO_3 for 30 min; lane 5, supernatant of the Na_2CO_3-treated membrane fraction after ultracentrifugation. MreB, which is a cytosolic protein, fractionates with the membrane and is retained in the membrane fraction after Na_2CO_3 treatment, which removes peripherally associated membrane proteins. MreB is removed from the membrane fraction after urea treatment (data not shown).

present in the supernatant (Fig. 4, lane 5). This result is consistent with the notion that a significant portion of MreB is polymerized, possibly as filaments, in *Caulobacter* cell extracts. In support of this, treatment with 6 M urea, which would solubilize polymerized MreB filaments, resulted in the disappearance of MreB from the pellet fraction (data not shown).

MreB depletion leads to a severe cell shape defect and cell death in Caulobacter

In *Caulobacter*, the *mreB* gene is the first gene in a 6.4 kb cluster encoding several known cell shape-determining genes, including *mreC*, *mreD*, *pbp2*, *rodA* and a gene encoding a conserved hypothetical protein. Initial attempts to generate an in frame deletion of *mreB* were unsuccessful, suggesting that *mreB* is an essential gene in *Caulobacter*. Similarly, a copy of *mreB* integrated into the xylose-inducible chromosomal *xylX* gene could not complement an in frame deletion in *mreB*, indicating that high levels of MreB may be required for survival of *Caulobacter*. Indeed, when *mreB* expression was driven by the xylose promoter from the low-copy plasmid pRK290, an in frame deletion (120 bp) of *mreB* could be generated (JG5000).

When JG5000 was grown in the presence of xylose (Figs 5A, 0 h), it possessed a wild-type phenotype. When these cells were grown in medium lacking xylose for 5 h, several cells increased in cell width (Fig. 5A, 5 h). After 10 h of growth in the absence of xylose, two cell types were predominant: expanded predivisional cells (Fig. 5A, cells labelled 'b') and large lemon-shaped cells (Fig. 5A, 10 h). The diameter of MreB depleted cells was significantly enlarged at the mid-cell. We also observed that, in some cells, the cytoplasmic membrane bulged out (Fig. 5A, 10 h, cells labelled 'a'), indicating that cell wall integrity was affected. If cells were depleted of MreB for more than 10 h, they began to lyse (data not shown), indicating that MreB is essential for cell wall synthesis and survival in *Caulobacter*. Immunoblot analysis of cell extracts indicated that MreB was nearly absent after 10 h of depletion (Fig. 5B). As MreB appeared to be involved in maintaining the rod-like shape of the cell, we examined the effect of changes in intracellular MreB concentrations

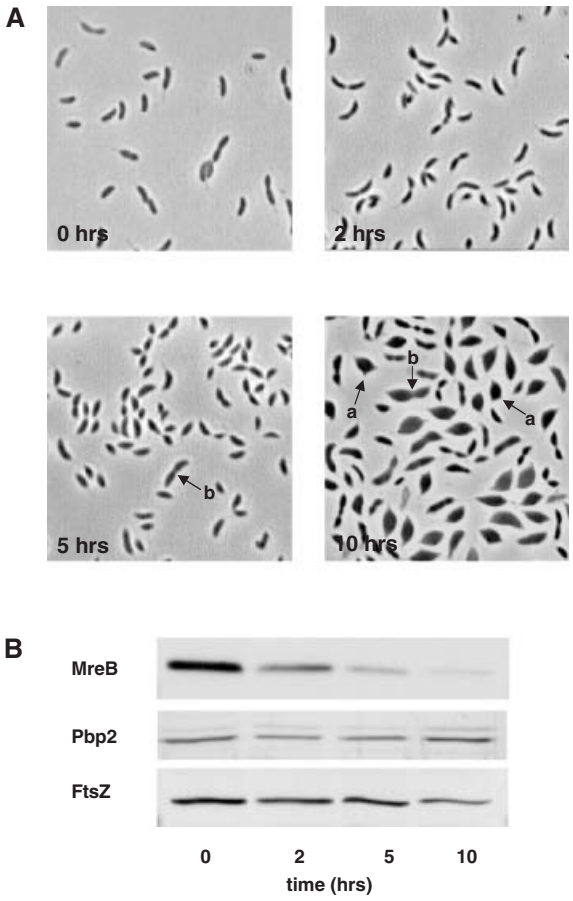

Fig. 5. MreB depletion results in defects in cell shape.
A. Cells of *C. crescentus* strain JG5000 containing a xylose-inducible allele of *mreB* and a deletion in the wild-type copy of the *mreB* gene were grown in the presence of xylose, washed three times in inducer-free medium and resuspended in fresh medium lacking inducer. Phase-contrast images were obtained before washing (0 h) and after 2, 5 and 10 h of incubation without inducer, as indicated. Loss of MreB results in an abundance of lemon-shaped cells, some of which have membrane blebs indicating a loss of cell wall integrity (cells labelled 'a'). Less abundant is the presence of other cells with defects in cell division (cells labelled 'b'). These cells possess a constriction at the mid-cell, as would occur if they arrested at the predivisional stage.
B. Cells of *C. crescentus* strain JG5000 were grown as described above. Samples were taken at the indicated time points and subjected to immunoblot analysis using polyclonal antibodies directed against MreB, FtsZ and PBP2.

on the amount of penicillin-binding protein 2 (PBP2), which has been shown in *E. coli* to be involved in cell wall synthesis along the long axis of the cell. Immunoblot analysis using anti-PBP2 antibody showed that PBP2 levels were not significantly affected by MreB depletion (Fig. 5B). Similarly, the levels of FtsZ, an early cell division protein, did not change significantly during the first 5 h of MreB depletion. However, after 10 h of depletion, the FtsZ levels decreased more significantly (Fig. 5B).

Penicillin-binding protein 2 (PBP2) localizes in a band-like pattern that is dependent on the presence of MreB

The cell wall defect exhibited by cells lacking MreB may be the result of unco-ordinated cell wall synthesis. A probable target for MreB activity is PBP2, which has been shown in *E. coli* to be required for the generation of rod-shaped cells. One hypothesis is that PBP2 might track along filaments of MreB, thus co-ordinating cell wall growth. In order to determine whether PBP2 exhibited a distinct subcellular localization pattern in *Caulobacter* cells, we raised antibody to a purified, truncated PBP2 containing the soluble periplasmic domain. Immunoblot analysis of whole-cell extracts revealed that this antibody reacted with two polypeptides of similar molecular weights (see Fig. 6A). This result was reminiscent of that observed previously for PBP2a and PBP2b when penicillin-binding proteins in *Caulobacter* extracts were separated by electrophoresis after labelling with radioactive penicillin (Koyasu *et al*., 1980; 1984; Nathan and Newton, 1988). In order to test whether these two immunoreactive bands were indeed PBP2a and PBP2b, we affinity labelled penicillin-binding proteins in whole-cell extracts of *Caulobacter* with fluorescein-tagged penicillin (Bocillin). After electrophoresis, the proteins were transferred to a nitrocellulose membrane and the gel scanned for fluorescein-tagged Bocillin. After scanning, the PBP-bound Bocillin was photobleached, and then the membrane was subjected to immunoblot analysis using anti-PBP2 antisera with CY3-conjugated antisera, and CY3 fluorescence was assayed. The scan for fluorescein-tagged Bocillin revealed several labelled polypeptides corresponding to the molecular masses of PBP1a, PBP1b, PBP2a, PBP2b, PBP3a, PBP3b as well as at least two other weakly labelled polypeptides of lower molecular weight (Fig. 6A). This pattern of labelled PBPs is similar to that observed previously for proteins labelled with radioactive penicillin (Koyasu

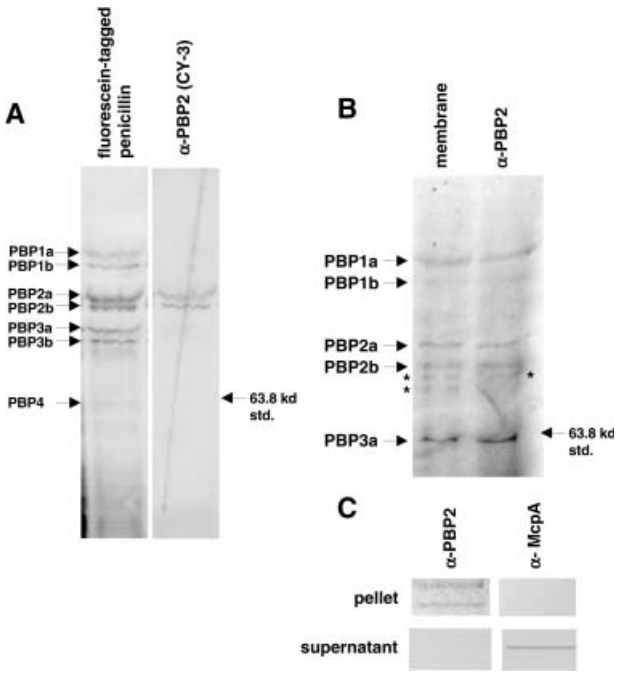

Fig. 6. Co-immunoprecipitation of PBP2 and other penicillin-binding proteins.
A. Cell extracts from mid-log phase *Caulobacter* cells were prepared, and the penicillin-binding proteins were labelled with fluorescein-tagged penicillin (Bocillin). Proteins in the extract were separated by SDS-PAGE (10% gel), transferred to nitrocellulose and the membrane analysed for fluorescein fluorescence (lane labelled: 'fluorescein-tagged penicillin'). The membrane was then photobleached and probed with anti-PBP2 antibody, which was detected with Cy3-conjugated secondary antibody (lane labelled αPBP2 (CY3)). This analysis reveals several polypeptides covalently bound to Bocillin including PBP1a, PBP1b, PBP2a, PBP2b, PBP3a, PBP3b and PBP4. This pattern is similar to previous results using radioactive penicillin to label PBPs in *Caulobacter* (Nathans and Newton, 1988). The PBP2 antibody recognized the two polypeptides corresponding to PBP2a and PBP2b. The migration of the fluorescently labelled 63.8 kDa molecular weight standard (BenchMark Prestained standards; Invitrogen) is indicated by an arrow.
B. Immunoprecipitation of PBP2 and other PBPs. Membranes were isolated from *Caulobacter* cells grown to mid-logarithmic phase and solubilized in dodecyl-maltoside (0.5%); the PBPs were labelled with the fluorescently labelled β-lactam, Bocillin. After low-speed centrifugation to remove aggregated material, the supernatants were mixed with anti-PBP2 antibody, the protein complexes were immunoprecipitated, subjected to electrophoresis (7.5% SDS–PAGE), and the fluorescently labelled protein was detected. Several fluorescently labelled PBPs were immunoprecipitated from membrane preparations with anti-PBP2 antibody (lane labelled α-PBP2). The PBPs present (PBP1a, PBP1b, PBP2a, PBP2b and PBP3a are numbered in order of descending molecular weight. Note that these numerical designations, with the exception of PBP2a and PBP3a, do not necessarily correlate in identity with the numerical designations of PBPs described in other organisms) in the membrane fraction before immunoprecipitation are also shown as a control. The labelled PBPs migrating between PBP2b and PBP3, designated with an '*', are probably proteolysed PBPs derived from higher molecular weight species. The migration of the fluorescently labelled 63.8 kDa molecular weight standard (BenchMark Prestained standards; Invitrogen) is indicated by an arrow.
C. The immunoprecipitated material in (B) was immunoblotted with antibodies directed against PBP2 or, as a control, the methyl-accepting chemotaxis receptor, McpA. Additionally, the material in the supernatants, following immunoprecipitation in (B), was subjected to immunoblotting with antibodies directed against PBP2 and the methyl-accepting chemotaxis receptor, McpA. McpA was not detected in the immunoprecipitation pellet, but was found in the supernatant. PBP2 is depleted from the supernatants after immunoprecipitation.

et al., 1980; 1984; Nathan and Newton, 1988). The immunoblot of the same membrane revealed that the PBP2 antibody reacted with polypeptides that appear to be identical in mass to labelled PBP2a and PBP2b (Fig. 6A).

We then performed an immunoprecipitation experiment with the PBP2 antibody using labelled membrane preparations. Membranes were isolated, solubilized in dodecylmaltoside (0.5%), and the PBPs were labelled with the fluorescein-tagged β-lactam, Bocillin. After low-speed centrifugation to remove aggregated material, the supernatants were mixed with antibody, the protein complexes were immunoprecipitated, subjected to electrophoresis and the fluorescently labelled protein was detected. Anti-PBP2 antibody immunoprecipitated Bocillin-labelled polypeptides corresponding to the molecular masses of PBP1a, PBP2a, PBP2b and PBP3a (Fig. 6B). The fact that several PBPs co-immunoprecipitated with anti-PBP2 antibody suggests that these penicillin-binding proteins form a complex *in vivo*. As a control, electrophoresis of the solubilized membrane preparation revealed the same labelled bands (Fig. 6B). In both the immunoprecipitated and solubilized membrane fractions, there were two to three additional labe-led bands of slightly smaller molecular weight than PBP2b (Fig. 6B) that were not present in the labelled whole-cell extracts (see Fig. 6A). We suspect that these are degradation products derived from higher molecular weight PBPs that accumulate during the membrane isolation procedure. [Also, note that PBP1b was barely detectable, and PBP3b was not detected in this isolated membrane fraction (Fig. 6B).] In order to verify that the anti-PBP2 antibody was not immunoprecipitating other membrane proteins or large fragments of membrane, we performed immunoblots on both the pellets and the depleted supernatants following immunoprecipitation. When anti-PBP2 antibody was used in the immunoprecipitation, PBP2 was present in association with the protein A–agarose pellet (Fig. 6C). Conversely, PBP2 was depleted from the supernatant of this immunoprecipitation reaction (Fig. 6C). PBP2 was not present in the pellets when anti-FtsZ (cytosolic protein) antibody (data not shown) or anti-McpA antibody (integral membrane protein) was used in the immunoprecipitation experiment (Fig. 6C). Taken together, these results indicate that PBP2 probably forms a complex with the other penicillin-binding proteins in *Caulobacter* cell membranes.

We then determined the subcellular localization pattern of PBP2 using immunofluorescence microscopy. In an unsynchronized population of cells, PBP2 foci appeared as discontinuous bands of globule-like foci perpendicular to the cell periphery and occurring along the entire cell length (Fig. 7A, 0 h). Deconvolution microscopy revealed that PBP2 localized as a series of stripes or bands along the length of the cell (Fig. 7B, a and b). We next investigated whether the pattern of PBP2 localization was dependent on the presence of MreB. Immunofluorescence microscopy on *Caulobacter* cells that had been depleted of MreB for 10 h demonstrated that PBP2 foci were still present in the absence of MreB. However, the distinct banding pattern was lost (Fig. 7A, 10 h, and B, c and d). Thus, PBP2 organization into the band-like pattern seems to be dependent on the presence of MreB. In order to determine whether PBP2 localization changed during the cell cycle in a fashion similar to MreB, we performed immunofluorescence microscopy on a synchronized *Caulobacter* population. In contrast to the MreB pattern of localization, there was no apparent concentration of PBP2 at the mid-cell halfway through the cell cycle (Fig. 7C). We found that the band-like organization of PBP2 globules was present along the length of the entire cell throughout the cell cycle.

Discussion

In this paper, we show that MreB plays an essential role in determining cell shape in *Caulobacter*. As cell shape in bacteria is attributed to the peptidoglycan cell wall, MreB most likely plays a role in co-ordinating the synthesis of peptidoglycan. Consistent with this idea, the depletion of MreB results in lemon-shaped cells (i.e. loss of rod-like shape) that possess defects in the integrity of the cell wall. MreB localization appears as bands or spirals that encircle the cell along its entire length. PBP2 also forms band-like structures that resemble MreB spirals. Recent experiments in *E. coli* have shown that PBP2–green fluorescent protein (GFP) fusions also exhibit a granular pattern of subcellular localization (den Blaauwen *et al*., 2003). In *Caulobacter*, localized PBP2 appears as granules organized as a series of bands or stripes, and this pattern of localization depends on the presence of MreB. We hypothesize that these granules of PBP2 may be viewed as peptidoglycan-synthesizing factories. Indeed, affinity chromatography has demonstrated that many of the PBPs in *E. coli* are present in a multienzyme complex (Schiffer and Holtje, 1999; Vollmer *et al*., 1999). Likewise, we have shown here that PBP2 antibody can immunoprecipitate other penicillin-binding proteins present in *Caulobacter* membrane preparations.

Daniel and Errington (2003) recently used fluorescently labelled vancomycin, an inhibitor of the transglycosylation reaction of peptidoglycan synthesis, to examine the topology of cell wall synthesis in *B. subtilis*. Vancomycin binding corresponds to sites of nascent peptidoglycan assembly. These experiments show that fluorescently labelled vancomycin localizes in a banded pattern along the long axis of the rod-shaped *B. subtilis* cell, reminiscent of the helical pattern exhibited by MreB. This helical pattern is dependent on the actin (MreB) homologue, Mbl. In *B. subtilis*, Mbl, like MreB, forms a spiral-like

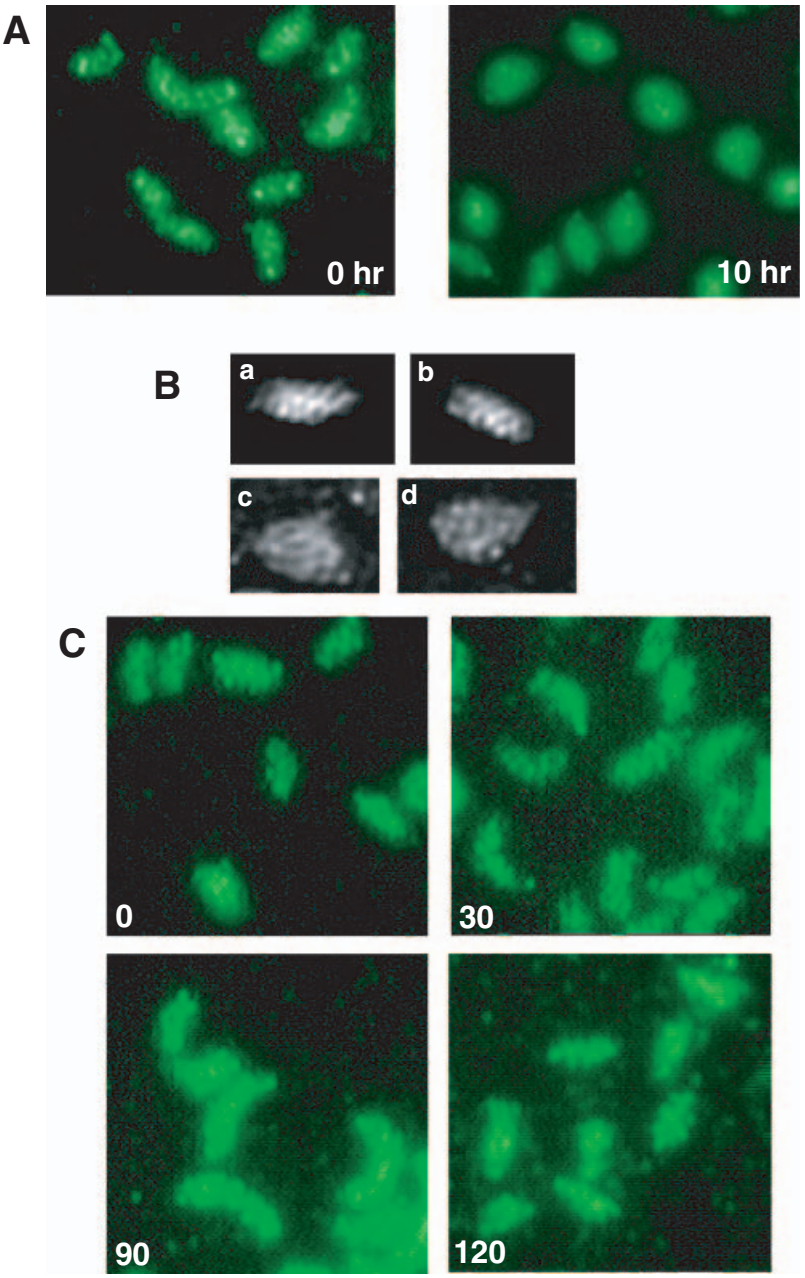

Fig. 7. Penicillin-binding protein 2 (PBP2) localizes in a banded pattern that is dependent on the presence of MreB.
A. The subcellular localization of penicillin-binding protein 2 (PBP2) was determined in the presence or absence of MreB. Cells of *C. crescentus* strain JG5000 were grown in PYE in the presence of 8 mM xylose. Before the removal of inducer (xylose), a sample was taken and processed for immunofluorescence microscopy. The cells were then depleted for MreB for 10 h, and another sample was processed for immunofluorescence microscopy. PBP2 localization was visualized by immunofluorescence microscopy using PBP2 antisera and Cy3-labelled secondary antibody. PBP2 staining is false-coloured green.
B. Deconvolution microscopy of PBP2 immunostaining. Images of wild-type cells after immunostaining of PBP2 (a and b) showing bands that are perpendicular to the cell border. This pattern is lost upon depletion of MreB (c and d).
C. Wild-type cells were grown in PYE, synchronized and allowed to proceed through the cell cycle. Samples were prepared for immunofluorescence microscopy at the indicated time points. Visualization of PBP2 was performed with immunofluorescence microscopy.

structure that assembles along the length of the cell (Jones *et al*., 2001). These results suggest that rod-shaped bacteria insert newly synthesized peptidoglycan in the pre-existing sacculus in a helical fashion. As the PBP2 pattern of localization in *Caulobacter* requires MreB, one reasonable hypothesis is that MreB filaments function as a cytoskeletal structure that serves as an organizer or a tracking device for the PBP2–peptidoglycan biosynthesis complex. A prediction of this hypothesis is that PBP factories would track along MreB spirals, thereby inserting peptidoglycan strands in a helical pattern that is somewhat perpendicular to the longitudinal axis of the cell.

In rod-shaped bacteria, cell elongation followed by cell division is accomplished by two distinct phases of synthesis of the murein sacculus (Wientjes and Nanninga, 1989; Nanninga, 1991; de Pedro *et al*., 1997). A recently divided bacterial cell will exhibit diffuse cell wall growth along the longitudinal axis. When the cell reaches a length that is approximately twice that of the newborn cell, sacculus growth is directed inwards at the mid-cell, culminating in the formation of a septum (Holtje, 1998). Two morphogenetic proteins, PBP2 and RodA, have been shown to play a critical role in the assembly of peptidoglycan along the long axis of the cell (Spratt, 1975; Tamaki *et al*., 1980; Begg and Donachie, 1985). Mutations in either gene

result in the loss of a rod shape and the formation spherical cells. Interestingly, PBP2 and RodA have homologues, PBP3 (*ftsI*) (Nakamura *et al*., 1983; Ishino *et al*., 1989) and FtsW (Khattar *et al*., 1994), that perform a similar function in peptidoglycan assembly at the nascent septum. MreB undergoes two distinct patterns of localization that change in a dynamic fashion during the cell cycle. During the cell elongation phase, MreB localization is observed along the length of the cell. At the initiation of cell division, localization appears to be concentrated at the mid-cell. Thus, this switch in localization pattern coincides with the switch from longitudinal growth to septal growth. We speculate that MreB has an integral role in co-ordinating the switch from longitudinal to septal peptidoglycan assembly. In support of this idea, MreB depletion, in addition to compromising the integrity of the peptidoglycan along the length of the cell, also causes a fraction of cells to arrest at the predivisional stage (see Fig. 5). Additionally, in *E. coli*, MreB mutants accumulate high levels of PBP3, indicating a possible connection between PBP3 and MreB (Wachi and Matsuhashi, 1989). It is likely that both peptidoglycan biosynthesis complexes involving PBP3 and PBP2 are co-ordinated through MreB spirals. Unlike MreB, the pattern of PBP2 localization did not concentrate to the mid-cell of predivisional cells in the experiments presented here. This may indicate that remaining longitudinal MreB spirals, those that do not move to a mid-cell location, are sufficient to maintain the PBP2 localization pattern.

The localization of MreB at mid-cell is dependant on the presence of FtsZ. The formation of FtsZ rings at the mid-cell is the earliest known cytological event in the initiation of cell division in bacteria. Furthermore, the FtsZ ring is required for the recruitment of other early cell division proteins, including FtsA, FtsQ, PBP3 and FtsW (Margolin, 2000). Using co-immunoprecipitation, we were not able to demonstrate experimentally a complex containing both FtsZ and MreB (data not shown). We hypothesize that MreB interacts with an early cell division protein, the localization of which at the mid-cell requires FtsZ. The cell cycle-regulated formation of the FtsZ ring would function in temporally regulating the mid-cell localization of this early cell division protein and subsequently, MreB.

It has been demonstrated that MreB folds into a structure and forms filaments that closely resemble actin (van den Ent *et al*., 2001), indicating that MreB and eukaryotic actin may share a common ancestor (Doolittle and York, 2002). In yeast, actin cables are required for the delivery of secretory vesicles and, thus, polarized growth (Pruyne and Bretscher, 2000). We speculate that MreB has a similar role in directing the co-ordinated insertion of peptidoglycan filaments into the bacterial cell wall. In eukaryotes, actin-binding proteins regulate actin assembly and disassembly (Pollard *et al*., 2000), which in turn leads to changes in cell shape. For example, profilin promotes actin assembly by maintaining a pool of ATP-bound actin that is ready to elongate actin filaments at the barbed end (Pollard *et al*., 2000). It is likely that the FtsZ-dependent localization of a critical cell division protein fulfils a similar function in regulating MreB assembly and disassembly at the mid-cell.

Experimental procedures

Strains and plasmids

All strains were derived from *Caulobacter crescentus* LS107 (Stephens *et al*., 1997). For the construction of the MreB depletion strain, a 797 bp fragment encompassing part of the *mreB* coding sequence (66 amino acids) and upstream region was amplified by polymerase chain reaction (PCR) and cloned into the *Nco*I and *Eco*RI site of pNPTS129 yielding plasmid pRF165. Additionally, a 799 bp fragment including part of the m*r*eB gene and of the intergenic region between *mreB* and *mreC* was amplified by PCR introducing an *Nco*I and *Xba*I site. This fragment was cloned into pRF165 resulting in a 102 bp deletion in the *mreB* coding sequence and creating plasmid pRF178, which was integrated into *Caulobacter*. Into this strain, we introduced plasmid pRF145, which is a derivative of pAA74 (R. M. Figge and J. W. Gober, unpublished) in which the *mreB* gene has been cloned downstream of the promoter of the *xylX* gene (Meisenzahl *et al*., 1997). Selection on peptone–yeast extract medium (PYE) containing 3% sucrose and 8 mM xylose yielded several mutants that had lost the pRF179-encoded *sacB* gene, thus creating an in frame deletion in *mreB*. Sucrose-insensitive mutants were tested for growth on media lacking xylose. The presence of the *mreB* in frame deletion in those colonies requiring xylose for growth was verified by PCR and subsequent digestion by *Nco*I, which cuts the *Nco*I site that had been introduced into the *mreB* gene together with the in frame deletion. The resulting conditional *mreB* mutant was called JG5000.

Immunofluorescence microscopy

For the generation of MreB and PBP2 antibodies, both genes were amplified by PCR. Oligonucleotides were used that resulted in the amplification of a portion of the *mreB* gene lacking the first 423 bp and *pbp2* lacking the first 603 bp, which encodes the membrane anchor domain. All fragments were cloned into pET28 (Novagen), and the corresponding 6× His-tagged proteins were purified using nickel-affinity chromatography. Antibodies were prepared by a commercial source (Cocalico) in rabbits. The MreB antibody was affinity purified using the Amino-Link Plus immobilization kit (Pierce).

For immunolocalization of MreB and penicillin-binding proteins, cells were grown to mid-log phase, fixed in 2.5% formaldehyde, 30 mM sodium phosphate (pH 7.4) for 15 min at 25°C and 45 min on ice. Cells were washed three times with PBS (140 mM NaCl, 3 mM KCl, 8 mM Na_2HPO_4 and 1.5 mM KH_2PO_4) and once with GTE (50 mM glucose, 10 mM EDTA, 20 mM Tris-HCl at pH 7.5) by filtration (0.45 μM; Millipore)

and suspended in GTE. Cells were treated with varying amounts of lysozyme (5–50 μg ml^{-1}), adhered to poly L-lysine-treated glass slides and dried completely. The slides were immersed in PBS, 2% bovine serum albumin (BSA) before incubating them with the appropriate primary antibody in the same buffer for 1 h. Slides were washed three times in PBS and incubated with secondary antibodies labelled with the fluorophore Cy-3 (Jackson Immunologicals) or Alexa 488 (Molecular Probes) for 1 h. Cells were washed three times in PBS and then covered by 60% glycerol containing 0.5 μg ml^{-1} 4,6-diamidino-2 phenylindole (DAPI) to stain DNA. In order to determine the percentage of MreB localized to the mid-cell, at least 100 cells each from two independent experiments were counted.

For conventional immunofluorescence, images were taken with an Optronics cooled CCD camera attached to a Zeiss Axioplan microscope at 1600× magnification. All images were captured with a PHOTOSHOP AV capture plug-in. For deconvolution microscopy, 15 images at 0.1 μm through the sample were collected with a Delta Vision (Applied Precision) optical sectioning microscope. These images were deconvolved using software from the manufacturer. Medial sections of the deconvolved images were imported into Adobe PHOTOSHOP.

Cell synchronization and depletion experiments

Caulobacter cells were synchronized essentially as described previously (Evinger and Agabian, 1977). *Caulobacter* was grown to an OD_{600} = 0.8–1.0 in PYE or M2 media. Cells were pelleted by centrifugation and suspended in ice-cold Percoll (Sigma) in M2 salts. The suspension was spun at 8500 *g*, and pure swarmer cells were isolated from the high-mobility band. These were washed twice in cold M2 salts and then suspended in prewarmed M2 or PYE and incubated at 31°C. At the indicated time points, samples were removed and labelled with 3 μCi ml^{-1} ^{35}S-*trans*-label (methionine, ICN Radiochemicals) for 10 min. Cell extracts were prepared, and labelled MreB was immunoprecipitated as described previously (Gomes and Shapiro, 1984) using affinity-purified MreB antibody.

Subcellular localization/polymerization of MreB

The protocol for the determination of the subcellular localization of MreB was derived from Hale and de Boer (1997). *Caulobacter* was grown to mid-log phase, cells were harvested, suspended in CBB buffer (20 mM Tris-HCl, pH 8.0, 25 mM NaCl, 5 mM EDTA, 3.6 mM 2-mercaptoethanol) and ruptured by a French pressure cell. Cellular debris was removed by centrifugation at 20 000 *g*, and membranes were isolated by centrifugation at 200 000 *g* for 1 h. The supernatant containing the cytosolic and periplasmic fractions was retained. The membrane pellet was suspended in CBB buffer by sonication and spun again for 1 h in a Beckman Coulter airfuge (≈ 100 000 *g*). To determine whether MreB was polymerized in the cytosol or membrane associated, washed membranes were suspended in 100 mM Na_2CO_3 (pH 11.4) and incubated on ice for 30 min. Then, the suspension was centrifuged again for 1 h at 100 000 *g*, the supernatant retained, and the pellet suspended in an equal volume of CBB buffer. Similarly, membranes were suspended in CBB with 6 M urea, pelleted again as above and suspended in CBB buffer. Proteins from equivalent portions of soluble and insoluble fractions were separated by SDS-PAGE gels and subjected to immunoblotting.

Immunoprecipitation of PBP complexes

Two litres of *C. crescentus* LS107 were grown to mid-log phase ($O.D_{600}$ 0.6–0.8) and harvested by centrifugation at 8500 *g*. The cells were washed with 25 ml of solubilization buffer (50 mM sodium phosphate, pH 7.4, 50 mM NaCl, 1 mM EDTA) three times and suspended to a final volume of 25 ml. The suspension was lysed in a French pressure cell at 1250 p.s.i. three times, whereupon phenylmethylsulphonyl fluoride (PMSF) was added to a final concentration of 1 mM. The resulting suspension was then centrifuged at 10 000 *g* for 15 min at 4°C and the supernatant collected. After centrifugation at 135 000 *g* for 1 h at 4°C, the membrane pellet was collected. After washing three times with solubilization buffer containing 0.5% dodecyl-maltoside, the pellets were suspended by sonication in the same buffer. The membranes were centrifuged in a tabletop centrifuge at 4000 *g* at 4°C for 10 min to remove insoluble membrane aggregates. The supernatant was then diluted to final total protein concentration of 30 mg ml^{-1}, using the Bio-Rad DC (detergent compatible) protein assay. Bocillin FL (Molecular Probes) in PBS with 30% ethanol was added to the solubilized membrane proteins to a final concentration of 30 μM.

The anti-PBP2 antibody was diluted 1:100 and incubated with the solubilized membrane proteins for 3 h at 4°C with gentle rocking. Then, 50 μl of protein A-coupled agarose (Pharmacia) equilibrated with solubilization buffer was added. After 1 h of continued incubation, the beads were centrifuged, the supernatant saved, and the beads washed with solubilization buffer containing 0.5% dodecyl-maltoside three times. The beads were suspended to a final volume of 100 μl, and a portion of the sample was subject to electrophoresis (7.5% SDS–PAGE) in the dark at 4°C. After electrophoresis, the gel was washed with distilled water and analysed on a Bio-Rad Molecular Imager FX with absorption at 488 nm and emission at 545 nm. In addition, a portion of the suspended immunoprecipitated material was saved for immunoblot analysis.

For the analysis of PBPs in *Caulobacter* cells, whole-cell extracts were prepared as described above, and Bocillin FL (Molecular Probes) in 100 mM sodium phosphate buffer, pH 7.5, was added to a final concentration to 30 μM**.** The sample was then incubated for 30 min at 30°C, subjected to SDS-PAGE on a 10% acrylamide gel and transferred to a nitrocellulose membrane. After incubation for 1 h in 20 mM Tris-HCl, pH 7.5, 500 mM NaCl (TBS) containing 5% BSA, the membrane was analysed on a Bio-Rad Molecular Imager FX with absorption at 488 nm and emission at 545 nm to obtain the PBP profile. The membrane was wrapped in cellophane and placed on an Image Eraser (Molecular Dynamics) for 1 h to bleach residual florescence and reanalysed on the Molecular Imager FX with absorption and emission at 488 nm/545 nm (fluorescein) and 550 nm/565 nm (CY3) with no detectable florescence. The membrane was then sub-

jected to immunoblotting with rabbit anti-PBP2 antibody. After washing, the membrane was incubated with secondary antibodies labelled with the fluorophore Cy-3 (Jackson Immunologicals). The membrane was again washed several times in TBS and visualized on the Molecular Imager with excitation at 550 nm and emission at 565 nm.

Acknowledgements

We are indebted to Kit Pogliano for use of the deconvolution microscope and help in analysing the data. We are grateful to Rachel Dutton for performing the deconvolution microscopy and data analysis. We appreciate helpful comments on the manuscript from R. Dutton, J. Easter, J. England, R. Muir and Z. Xu. R.M.F. acknowledges the receipt of an EMBO long-term fellowship. This work was supported by grants from the National Science Foundation (MCB-9986127) and the National Institutes of Health (GM48147) to J.W.G.

References

Begg, K.J., and Donachie, W.D. (1985) Cell shape and division in *Escherichia coli*: experiments with shape and division mutants. *J Bacteriol* **163:** 615–622.

den Blaauwen, T., Aarsman, M.E.G., Vischer, N.O.E., and Nanninga, N. (2003) Penicillin-binding protein PBP2 of *Escherichia coli* localizes preferentially in the lateral wall and at the mid-cell in comparison with the old cell pole. *Mol Microbiol* **47:** 539–547.

Daniel, R.A., and Errington, J. (2003) Control of cell morphogenesis in bacteria: two distinct ways to make a rod-shaped cell. *Cell* **113:** 767–776.

Doi, M., Wachi, M., Ishino, F., Tomioka, S., Ito, M., Sakagami, Y., *et al.* (1988) Determinations of the DNA sequence of the mreB gene and of the gene products of the mre region that function in formation of the rod shape of *Escherichia coli* cells. *J Bacteriol* **170:** 4619–4924.

Doolittle, R.F., and York, A.L. (2002) Bacterial actins? An evolutionary perspective. *Bioessays* **24:** 293–296.

van den Ent, F., Amos, L.A., and Lowe, J. (2001) Prokaryotic origin of the actin cytoskeleton. *Nature* **413:** 39–44.

Evinger, M., and Agabian, N. (1977) Envelope-associated nucleoid from *Caulobacter crescentus* stalked and swarmer cells. *J Bacteriol* **132:** 294–301.

Gomes, S.L., and Shapiro, L. (1984) Differential expression and positioning of chemotaxis methylation proteins in *Caulobacter*. *J Mol Biol* **178:** 551–568.

Hale, C.A., and de Boer, P.A. (1997) Direct binding of FtsZ to ZipA, an essential component of the septal ring structure that mediates cell division in *E. coli*. *Cell* **88:** 175–185.

Holtje, J.V. (1998) Growth of the stress-bearing and shape-maintaining murein sacculus of *Escherichia coli*. *Microbiol Mol Biol Rev* **62:** 181–203.

Ishino, F., Jung, H.K., Ikeda, M., Doi, M., Wachi, M., and Matsuhashi, M. (1989) New mutations fts-36, lts-33, and ftsW clustered in the mra region of the *Escherichia coli* chromosome induce thermosensitive cell growth and division. *J Bacteriol* **171:** 5523–5530.

Jones, L.J., Carballido-Lopez, R., and Errington, J. (2001) Control of cell shape in bacteria: helical, actin-like filaments in *Bacillus subtilis*. *Cell* **104:** 913–922.

Kelly, A.J., Sackett, M.J., Din, N., Quardokus, E., and Brun, Y.V. (1998) Cell cycle-dependent transcriptional and proteolytic regulation of FtsZ in *Caulobacter*. *Genes Dev* **12:** 880–893.

Khattar, M.M., Begg, K.J., and Donachie, W.D. (1994) Identification of FtsW and characterization of a new ftsW division mutant of *Escherichia coli*. *J Bacteriol* **176:** 7140–7147.

Koehler, C.M., Jarosch, E., Tokatlidis, K., Schmid, K., Schweyen, R.J., and Schatz, G. (1998) Import of mitochondrial carriers mediated by essential proteins of the intermembrane space. *Science* **279:** 369–373.

Koyasu, S., Fukuda, A., and Okada, Y. (1980) The penicillin-binding proteins of *Caulobacter crescentus*. *J Biochem* **87:** 363–366.

Koyasu, S., Fukuda, A., and Okada, Y. (1984) Alteration in penicillin-binding patterns during the cell cycle of *Caulobacter crescentus*. *J Biochem* **95:** 593–595.

Levin, P.A., Margolis, P.S., Setlow, P., Losick, R., and Sun, D. (1992) Identification of *Bacillus subtilis* genes for septum placement and shape determination. *J Bacteriol* **174:** 6717–6728.

Margolin, W. (2000) Themes and variations in prokaryotic cell division. *FEMS Microbiol Rev* **24:** 531–548.

Meisenzahl, A.C., Shapiro, L., and Jenal, U. (1997) Isolation and characterization of a xylose-dependent promoter from *Caulobacter crescentus*. *J Bacteriol* **179:** 592–600.

Mohl, D.A., and Gober, J.W. (1997) Cell cycle-dependent polar localization of chromosome partitioning proteins in *Caulobacter crescentus*. *Cell* **88:** 675–684.

Nakamura, M., Maruyama, I.N., Soma, M., Kato, J., Suzuki, H., and Horota, Y. (1983) On the process of cellular division in *Escherichia coli*: nucleotide sequence of the gene for penicillin-binding protein 3. *Mol Gen Genet* **191:** 1–9.

Nanninga, N. (1991) Cell division and peptidoglycan assembly in *Escherichia coli*. *Mol Microbiol* **5:** 791–795.

Nathans, P., and Newton, A. (1988) Identification of two new cell division genes that affect a high-molecular-weight penicillin-binding protein in *Caulobacter crescentus*. *J Bacteriol* **170:** 2319–2327.

de Pedro, M.A., Quintela, J.C., Holtje, J.V., and Schwarz, H. (1997) Murein segregation in *Escherichia coli*. *J Bacteriol* **179:** 2823–2834.

Pollard, T.D., Blanchoin, L., and Mullins, R.D. (2000) Molecular mechanisms controlling actin filament dynamics in nonmuscle cells. *Annu Rev Biophys Biomol Struct* **29:** 545–576.

Pruyne, D., and Bretscher, A. (2000) Polarization of cell growth in yeast. I. Establishment and maintenance of polarity states. *J Cell Sci* **113:** 365–375.

Satta, G., Canepari, P., Botta, G., and Fontana, R. (1980) Control of cell septation by lateral wall extension in a pH-conditional morphology mutant of *Klebsiella pneumoniae*. *J Bacteriol* **142:** 43–51.

Schiffer, G., and Holtje, J.V. (1999) Cloning and characterization of PBP 1C, a third member of the multimodular class A penicillin-binding proteins of *Escherichia coli*. *J Biol Chem* **274:** 32031–32039.

Shih, Y.L., Le, T., and Rothfield, L. (2003) Division site selec-

tion in *Escherichia coli* involves dynamic redistribution of Min proteins within coiled structures that extend between the two cell poles. *Proc Natl Acad Sci USA* **100:** 7865–7870.

Spratt, B.G. (1975) Distinct penicillin-binding proteins involved in the division, elongation, and shape of *Escherichia coli* K12. *Proc Natl Acad Sci USA* **72:** 2999–3003.

Spratt, B.G., and Pardee, A.B. (1975) Penicillin-binding proteins and cell shape in *E. coli*. *Nature* **275:** 516–517.

Stephens, C., Mohr, C., Boyd, C., Maddock, J., Gober, J., and Shapiro, L. (1997) Identification of the fliI and fliJ components of the *Caulobacter* flagellar type III protein secretion system. *J Bacteriol* **179:** 5355–5365.

Tamaki, S., Matsuzawa, H., and Matsuhashi, M. (1980) Cluster of mrdA and mrdB genes responsible for the rod shape and mecillinam sensitivity of *Escherichia coli*. *J Bacteriol* **141:** 52–57.

Varley, A.W., and Stewart, G.C. (1992) The divIVB region of the *Bacillus subtilis* chromosome encodes homologs of *Escherichia coli* septum placement (minCD) and cell shape (mreBCD) determinants. *J Bacteriol* **174:** 6729–6742.

Vollmer, W., von Rechenberg, M., and Holtje, J.V. (1999) Demonstration of molecular interactions between the murein polymerase PBP1B, the lytic transglycosylase MltA, and the scaffolding protein MipA of *Escherichia coli*. *J Biol Chem* **274:** 6726–6734.

Wachi, M., and Matsuhashi, M. (1989) Negative control of cell division by mreB, a gene that functions in determining the rod shape of *Escherichia coli* cells. *J Bacteriol* **171:** 3123–3127.

Wachi, M., Doi, M., Tamaki, S., Park, W., Nakajima-Iijima, S., and Matsuhashi, M. (1987) Mutant isolation and molecular cloning of mre genes, which determine cell shape, sensitivity to mecillinam, and amount of penicillin-binding proteins in *Escherichia coli*. *J Bacteriol* **169:** 4935–4940.

Wang, Y., Jones, B.D., and Brun, Y.V. (2001) A set of ftsZ mutants blocked at different stages of cell division in *Caulobacter*. *Mol Microbiol* **40:** 347–360.

Wientjes, F.B., and Nanninga, N. (1989) Rate and topography of peptidoglycan synthesis during cell division in *Escherichia coli*: concept of a leading edge. *J Bacteriol* **171:** 3412–3419.